again we must conclude that the temperature derivative of the shear modulus must be at least three times that of the bulk modulus.

Whereas the absolute value of the mantle shear modulus can be reconciled by much higher temperatures than we assumed or by a lower mantle Fe/Fe+Mg ratio of at least 0.3, the only conclusion that is also consistent with the seismic tomography is that the lower mantle exhibits an unusually large apparent temperature derivative of the shear modulus as compared to that of the bulk modulus. Recent workers have calculated (*16*) that this ratio cannot exceed unity if perovskite behaves as a normal refractory ceramic with a close-packed oxygen framework. A ferroelastic phase transformation could allow the effective temperature derivative of the shear modulus to be very large, which would account for all of these observations. Such a large negative value will result if the mantle temperature is sufficiently close to that required for a ferroelastic-paraelastic phase transformation in the perovskite phase, so as to induce significant shear mode softening. These transformations are common in perovskite-type compounds and have been predicted theoretically for $MgSiO_3$ (*17*). These phase transformations typically have shallow Clapeyron slopes that could conceivably be parallel to the geothermal gradient. Because other physical properties, including thermal expansion and rheology, will be affected by these transformations, we need to broaden our understanding of this phenomena to determine the physical and chemical properties of the earth's lower mantle.

REFERENCES AND NOTES

1. L. G. Liu, *Nature* **258**, 770 (1976); A. E. Ringwood, *J. Geophys. Res.* **67**, 4005 (1962); E. Ito, E. Takahashi, Y. Matsui, *Earth Planet. Sci. Lett.* **67**, 283 (1984); E. Ito and H. Yamada, in *High Pressure Research in Geophysics*, S. Akimoto and M. H. Manghnani, Eds. (Center for Academic Publishing, Tokyo, 1982), pp. 405–419; T. Yagi, H-K. Mao, P. M. Bell, *Carnegie Inst. Washington Yearb.* **614**, 78 (1979); E. Ito and Y. Matsui, *Earth Planet. Sci. Lett.* **38**, 443 (1978).
2. H. D. Megaw, *Crystal Structures: A Working Approach* (Saunders, Philadelphia, 1973); A. H. Glazer, *Acta Crystallogr. Sec. B* **28**, 3384 (1972); *ibid. Sec. A* **31**, 756 (1975).
3. H. D. Megaw, *Acta Crystallogr.* **5**, 739 (1952); R. Rao and K. J. Rao, *Phase Transitions in Solids* (McGraw-Hill, New York, 1977); J. B. Goodenough and J. M. Longo, in *Landolt-Bornstien New Series, Group III* (Springer-Verlag, Berlin, 1970), vol. 4A, pp. 125–315.
4. Brillouin spectroscopy provides an optical method for measuring acoustic velocities as a function of crystallographic direction in single crystals. Laser light that passes through the sample is Doppler-shifted by the thermally generated acoustic waves. The acoustic velocity is inferred from the measured frequency shift of the scattered light. We are able to determine these properties on single crystals as small as 50 μm, thus allowing these properties to be determined on materials synthesized at high pressure. For additional details of the technique, see D. J. Weidner and H. R. Carleton, *J. Geophys. Res.* **82**, 1334 (1977); D. J. Weidner and M. T. Vaughan, in *High Pressure Science and Technology*, D. Timmerhaus and M. S. Barber, Eds. (Plenum, New York, 1979), vol. 2, pp. 85–90; M. T. Vaughan and J. D. Bass, *Phys. Chem. Minerals* **10**, 62 (1983).
5. E. Ito and D. J. Weidner, *Geophys Res. Lett.* **13**, 464 (1986).
6. D. J. Weidner and E. Ito, *Phys. Earth Planet. Inter.* **40**, 64 (1985); ———, J. D. Bass, A. E. Ringwood, W. Sinclair, *J. Geophys. Res.* **87**, 4740 (1982).
7. R. E. Cohen, *Geophys. Res. Lett.* **14**, 1053 (1987).
8. T. Yagi, H. K. Mao, P. M. Bell, in *Advances in Physical Geochemistry*, S. Saxina, Ed. (Springer-Verlag, New York, 1982), vol. 2, pp. 317–325.
9. E. Knittle and R. Jeanloz, *Science* **235**, 668 (1987).
10. Y. Kudoh, E. Ito, H. Takeda, *Phys. Chem. Minerals* **14**, 350 (1987).
11. K. Aizu, *J. Phys. Soc. Jpn.* **28**, 706 (1970); J. Sapriel, *Phys. Rev. B* **12**, 5128 (1975).
12. S. C. Abrahams, J. L. Bernstein, J. P. Remeika, *Mater. Res. Bull.* **9**, 1613 (1974); ———, R. L. Burns, J. L. Bernstein, *Solid State Commun.* **10**, 379 (1972).
13. R. M. Hazen and N. L. Ross, *Eos* **69**, 473 (1988).
14. A. M. Dziewonski and D. L. Anderson, *Phys. Earth. Planet. Inter.* **25**, 297 (1981).
15. J. H. Woodhouse, A. M. Dziewonski, D. Giardini, X. D. Li, A. Morelli, *Eos* **68**, 356 (1987).
16. O. L. Anderson, T. Goto, D. Isaak, *ibid.*, p. 1488 (1987); E. K. Graham and E. G. Hilbert, *ibid.* **69**, 472 (1988).
17. G. H. Wolf and M. S. T. Bukowinski, in *High Pressure Research in Mineral Physics*, M. H. Manghnani and Y. Syono, Eds. (Terra Scientific, Tokyo, and American Geophysical Union, Washington, DC, 1987), pp. 315–331.

18. This research was supported by NSF grant EAR-85942755.

8 August 1988; accepted 16 December 1988

The Manganese Site of the Photosynthetic Water-Splitting Enzyme

GRAHAM N. GEORGE, ROGER C. PRINCE, STEPHEN P. CRAMER

As the originator of the oxygen in our atmosphere, the photosynthetic water-splitting enzyme of chloroplasts is vital for aerobic life on the earth. It has a manganese cluster at its active site, but it is poorly understood at the molecular level. Polarized synchrotron radiation was used to examine the x-ray absorption of manganese in oriented chloroplasts. The manganese site, in the "resting" (S_1) state, is an asymmetric cluster, which probably contains four manganese atoms, with interatomic separations of 2.7 and 3.3 angstroms; the vector formed by the 3.3-angstrom manganese pair is oriented perpendicular to the membrane plane. Comparisons with model compounds suggest that the cluster contains bridging oxide or hydroxide ligands connecting the manganese atoms, perhaps with carboxylate bridges connecting the 3.3-angstrom manganese pair.

DESPITE EXTENSIVE STUDIES BY X-ray (*1–3*), electron paramagnetic resonance (EPR) (*4*), and optical spectroscopies (*5*), the structure of the manganese (Mn) center of the water-splitting enzyme remains unknown. The enzyme is located in the thylakoid membrane, and during turnover it donates electrons to photosystem II, which are then recovered by the oxidation of H_2O to liberate oxygen (*6*). The enzyme cycles among five different oxidation levels, known as the *S* states, S_0 through S_4, which are thought to be reflections of different oxidation levels of a multinuclear Mn cluster (*6*). X-ray absorption spectroscopy should be capable of providing a detailed picture of the Mn environment, but, despite much effort (*1–3*), many questions remain.

Experiments were performed at the Stanford Synchrotron Radiation Laboratory on beam lines VI-2 and IV-2 with Si(400) double-crystal monochromators. X-ray absorption was monitored as the x-ray fluorescence excitation spectrum by means of an array of 13 germanium detectors (*7*), with simultaneous measurement of a Mn foil standard [first inflection, 6539.0 eV (*8*)]. Samples were kept dark at 4 K in an Oxford Instruments CF1204 cryostat during data collection. A typical data set (one orientation) represents the average of four to ten scans, each 20 minutes in duration. The oriented spinach chloroplast membranes (*9*) gave no adventitious Mn EPR signals and showed full photoactivity within the reaction centers and their associated redox partners (*9*). Samples were in the dark-adapted S_1 state, and their integrity and orientation were routinely assessed by EPR spectroscopy.

The extended x-ray absorption fine structure (EXAFS) oscillations $\chi(k)$ for individual orientations were fitted by standard methods (*10, 11*). For oriented systems, the EXAFS intensity is approximately proportional to $\cos^2\beta$, where β is the angle between the x-ray electric field vector, **e**, and the absorber-backscatterer vector. Transitions to bound states of predominantly *p* character have a similar angular dependence, where β is the angle between the axis of the

G. N. George and R. C. Prince, EXXON Research and Engineering Company, Annandale, NJ 08801.
S. P. Cramer, Schlumberger-Doll Research, Ridgefield, CT 06877.

p orbital and the x-ray **e** vector [see (*12*) for example]. Approximating the effects of sample disorder by a Gaussian distribution of orientations, we found that $F_{ab}(\theta)$ is given by

$$F_{ab}(\theta) = 3\left[\int_{\phi=0}^{\pi}(\tfrac{1}{2}\sin^2\theta\sin^2\phi + \cos^2\theta\cos^2\phi)\,P(\phi)\,d\phi\right]\Big/\int_{\phi=0}^{\pi}P(\phi)\,d\phi \quad (1)$$

where ϕ_{ab} is the angle between the membrane normal and the a–b vector (or the axis of the orbital for transitions to p levels), θ is the experimentally varied angle between the membrane normal and the x-ray **e** vector, Ω is the half-width of the Gaussian distribution in ϕ_{ab}, and

$$P(\phi) = \sin\phi\,\exp[-(\ln 2)\,(\phi - \phi_{ab})^2/\Omega^2]$$

Equation 1 was solved numerically with a value for Ω of 17° obtained from EPR measurements.

Several features of the Mn K edge show subtle but well-defined dichroism (Fig. 1a). All the spectra exhibited a small $1s\rightarrow 3d$ transition at about 6540.8 eV. Such formally dipole-forbidden transitions gain intensity by the mixing of $3d$ and $4p$ levels or through a quadrupole mechanism (*13*). Tetrahedral complexes exhibit intense $1s\rightarrow 3d(T_2)$ transitions because of extensive p-d mixing (*14*). The weak $1s\rightarrow 3d$ transition suggests that the Mn sites do not approach tetrahedral geometry. Some angular dependence of the $1s\rightarrow 3d$ feature is apparent, the shape changing from a shoulder-like structure at 90° to an isolated peak at 15°. Furthermore, the features at 6557 and 6564 eV at 15° are replaced by a single broad feature at 6560 eV at 90°. Although a quantitative interpretation of these spectra must await single-crystal data from model compounds, the presence of such well-defined dichroism indicates unambiguously that the Mn cluster in the S_1 state is highly oriented within the membrane but is not a highly symmetric structure such as a cube.

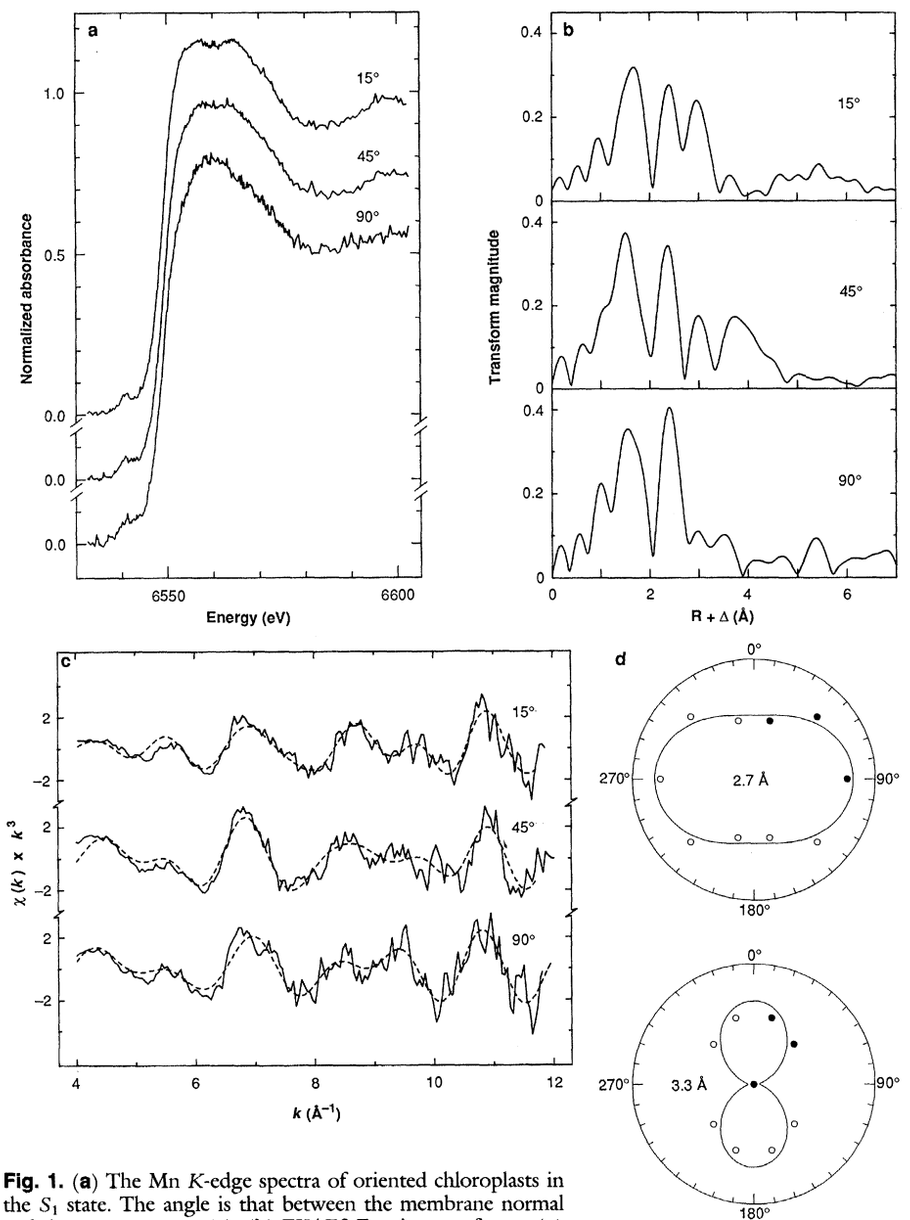

Fig. 1. (**a**) The Mn K-edge spectra of oriented chloroplasts in the S_1 state. The angle is that between the membrane normal and the x-ray **e** vector (θ). (**b**) EXAFS Fourier transforms. (**c**) Unsmoothed EXAFS data (solid lines), with best fits (broken lines) (Table 1). (**d**) Polar plots of the EXAFS amplitudes derived from the curve fitting of (c). Filled points are the experimental data, which have been mirrored for clarity as the open symbols. The curves represent best fits to Eq. 1, with 2.1 and 0.8 Mn–Mn vectors at average angles of 62° and 0° for 2.7 Å and 3.3 Å interactions, respectively.

The peak in the EXAFS Fourier transform (Fig. 1b) at a radial coordinate $R + \Delta = 1.6$ Å is attributable to interactions of Mn with oxygen or nitrogen, Mn–O or Mn–N (*15*), at an average distance of 1.9 Å, whereas the features at $R + \Delta = 2.4$ and 3.0 Å are attributable to Mn–Mn interactions at 2.7 and 3.3 Å, respectively (Fig. 1c and Table 1). No interactions of Mn with sulfur or chlorine are apparent, although a small contribution from such ligands (for example, 1 per 4 Mn atoms) is difficult to exclude.

The Mn–O and Mn–N interactions exhibit little angular dependence (Table 1). On the other hand, the Mn–Mn interactions show significant dichroism, especially the 3.3 Å Mn–Mn interaction, which is intense at 15° and weak at 90°. The 3.3 Å Mn–Mn vector is thus oriented close to the membrane normal. The fits (Fig. 1d) (*16*) suggest 2.1 ± 1 and 0.8 ± 0.3 Mn–Mn vectors (per Mn) oriented at average angles of approximately 62° and 0° for the 2.7 Å and 3.3 Å interactions, respectively (*16*). An additional interaction, indicated by the peak at $R + \Delta = 3.8$ Å in the EXAFS Fourier transform for $\theta = 45°$ (Fig. 1b), displays an orientation dependence that is not explained by Eq. 1. We conclude that it arises from a process whose amplitude does not depend simply on $\cos^2\beta$, such as multiple scattering (*17*).

Our interpretations contrast in some respects with those reported by Klein and colleagues (*1–3*) from unoriented samples. Whereas they reported very intense EXAFS from short Mn–O and Mn–N interactions at 1.75 Å, we find no evidence for such interactions (*18*). Nevertheless, in agreement with our results, Klein and co-workers did detect the 2.7 Å Mn–Mn interaction (*1–3*), and Guiles *et al.* have reported some evidence for the 3.3 Å Mn–Mn interaction (*2*).

Although it is not possible to deduce an unambiguous structure for the active site from the present data, some structural ele-

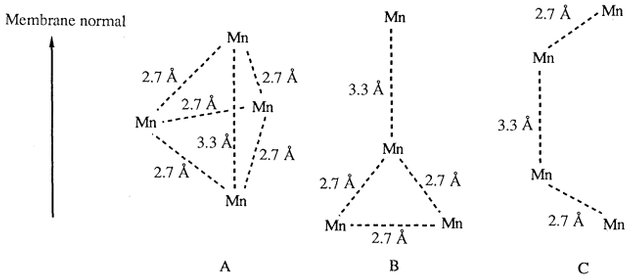

Fig. 2. Possible geometries of the Mn site consistent with both the polarization and the amplitudes of the Mn–Mn interactions. Note that versions B and C have Mn–Mn vectors at >3.3 Å, which might have escaped detection. The number of 2.7 Å Mn–Mn interactions in version C is just outside the estimated error range, but we include it for comparison.

Mn–Mn	2.7 Å		3.3 Å	
	N	$<\phi>$	*N*	$<\phi>$
Experimental	2.1±0.8	62°	0.8±0.3	0°
A	2.5	57°	0.5	0°
B	1.5	45°	0.5	0°
C	1.0	62°	0.5	0°

Table 1. EXAFS curve-fitting results. As both $F(\theta)$ and N are unknown quantities and because there are several Mn atoms in the cluster, the usual method of holding N at integer values during fitting was not used. The Debye-Waller factor σ_{ab} was fixed at the chemically reasonable values of 0.059 Å for Mn–O interactions and 0.077 Å for Mn-Mn interactions. The values of R have an accuracy [arising predominantly from nontransferability of $\alpha_{ab}(k)$] of ±0.03 Å, although the k range dictates a resolution of ≈0.14 Å for interactions with similar atoms.

Angle	Mn–O[1]		Mn–O[2]		Mn–Mn[1]		Mn–Mn[2]	
	$F(\theta)\cdot N$	*R* (Å)	$F(\theta)\cdot N$	*R* (Å)	$F(\theta)\cdot N$	*R* (Å)	$F(\theta)\cdot N$	*R* (Å)
15°	0.9	1.897	1.0	2.218	1.5	2.701	1.7	3.298
45°	1.2	1.895	0.6	2.270	2.2	2.722	1.4	3.255
90°	1.0	1.896	1.0	2.207	2.3	2.727	0.0	

ments are clear. The apparently low number of Mn–O and Mn–N ligands (2 ± 1, Table 1) is probably the result of a broad and non-Gaussian distribution of different distances rather than a truly low coordination number (*19*). Such a distribution might reflect a significant fraction of high-spin Mn(III) in the cluster because pronounced Jahn-Teller effects are expected for this oxidation state (*20*). Although we cannot distinguish between Mn–O and Mn–N interactions, a predominance of Mn–O seems most probable, especially for the bridging ligands (*20*).

The observed Mn–Mn interactions probably originate from bridged atoms, because EXAFS from unconnected Mn should be heavily damped by static and thermal disorder. Plausible bridging ligands include oxo, hydroxo, alkyl and aryloxide (tyrosine, for instance), and carboxylate (*20*). The Mn–Mn distance of 2.7 Å is symptomatic of more than one short bridging ligand between the Mn atoms concerned (*20*) and indicates that at least some portion of the cluster must be quite compact. The 2.7 Å Mn–Mn separation has been taken as evidence for μ_2-oxo bridges (*1–3*), but μ_3-oxo or μ_2-OH bridges are equally probable (*20*). The presence of μ_2-OH ligands gains support from EPR spectroscopy of the "multiline" signal of the S_2 state (*4*), which indicates the presence of exchangeable oxygen and protons (*21*). The 3.3 Å Mn–Mn separation is typical of Mn separated by two carboxylate bridges and a bridging oxo (μ_2 or μ_3); μ_2-OH or μ_2-OR groups are also plausible, although the latter tend to give Mn–Mn separations larger than 3.3 Å (*20*).

Proposals for the structure of the Mn site in the S_1 state include a regular cube (*22*) and a "butterfly" structure (*23*), both with μ_3-oxo bridges. Although both of these proposals are excluded by our data, more distorted versions are permissible. Three alternative geometries for the Mn cluster, consistent with our results, are suggested in Fig. 2.

REFERENCES AND NOTES

1. J. A. Kirby, D. B. Goodin, T. Wydrzynski, A. S. Robertson, M. P. Klein, *J. Am. Chem. Soc.* **103**, 5537 (1981).
2. R. D. Guiles *et al.*, in *Progress in Photosynthesis Research*, J. Biggins, Ed. (Nijhoff, Dordrecht, 1987), vol. 1, pp. 561–564.
3. V. K. Yachandra *et al.*, *Biochemistry* **26**, 5974 (1987); A. E. McDermott *et al.*, *ibid.* **27**, 4021 (1988).
4. G. C. Dismukes and Y. Siderer, *Proc. Natl. Acad. Sci. U.S.A.* **78**, 274 (1981); J. C. De Paula, W. F. Beck, A.-F. Miller, R. B. Wilson, G. W. Brudvig, *J. Chem. Soc. Faraday Trans. 1* **83**, 3635 (1987).
5. J. Lavergne, *Biochim. Biophys. Acta* **894**, 91 (1987).
6. R. C. Prince, *Trends Biochem. Sci.* **11**, 491 (1986); G. W. Brudvig, *J. Bioenerg. Biomembranes* **19**, 91 (1987).
7. S. P. Cramer, O. Tench, M. Yocum, G. N. George, *Nucl. Instrum. Methods Phys. Res. A* **266**, 586 (1988).
8. J. A. Bearden and A. F. Burr, *Rev. Mod. Phys.* **39**, 125 (1967).
9. R. C. Prince *et al.*, *Biochim. Biophys. Acta* **592**, 323 (1980); M. S. Crowder, R. C. Prince, A. J. Bearden, *FEBS Lett.* **144**, 204 (1982); A. W. Rutherford, *Biochim. Biophys. Acta* **807**, 189 (1985).
10. The EXAFS oscillations $\chi(k)$ were fitted to the approximate relation:

$$\chi(k) \simeq \sum_b \frac{F_{ab}(\theta)\, N_b A_{ab}(k)}{kR_{ab}^2} \times e^{-2\sigma_{ab}^2 k^2} \sin[2kR_{ab} + \alpha_{ab}(k)]$$

where k is the photoelectron wave vector, N_b is the number of b type atoms at a distance R_{ab} from the absorber atom a with a root-mean-square deviation σ_{ab} (the Debye-Waller factor) in R_{ab}; $A_{ab}(k)$ and $\alpha_{ab}(k)$ are the total phase shift and amplitude functions, respectively; and $F_{ab}(\theta)$ is the observed angular dependence of the EXAFS amplitude. Values for the functions $A_{ab}(k)$ and $\alpha_{ab}(k)$ were calculated [P. M. Eisenberger, R. G. Shulman, B. M. Kinkaid, G. S. Brown, S. Ogawa, *Nature* **224**, 30 (1978)] from $KMnO_4$ [G. J. Palenik, *Inorg. Chem.* **18**, 503 (1967)] and $[(C_6H_{15}N_3)_4Mn_4O_6](ClO_4)_4$ [K. Weighardt, U. Bossel, W. Gebert, *Angew. Chem. Int. Ed. Engl.* **22**, 328 (1983)]. A value for σ_{ab} of 0.0406 Å was calculated for $KMnO_4$ from the vibrational spectra. We estimated values for σ_{ab} for $[(C_6H_{15}N_3)_4Mn_4O_6](ClO_4)_4$ by fitting $A_{ab}(k)$ to interpolated theoretical values (*11*) with an adjustable scaling factor and adjusting σ_{ab}.
11. B.-K. Teo and P. A. Lee, *J. Am. Chem. Soc.* **101**, 2815 (1979).
12. T. A. Smith *et al.*, *ibid.* **107**, 5945 (1985).
13. J. E. Hahn *et al.*, *Chem. Phys. Lett.* **88**, 595 (1982).
14. R. G. Shulman *et al.*, *Proc. Natl. Acad. Sci. U.S.A.* **73**, 1384 (1976).
15. Typical values for Δ in EXAFS Fourier transforms are 0.3 to 0.5 Å. Note that EXAFS cannot distinguish between interactions with atoms of similar atomic number, such as nitrogen and oxygen.
16. It is not possible to obtain individual ϕ_{ab} values (Eq. 1) when there is more than one scatterer of a given type at similar distances. Nevertheless, an average value $\langle\phi\rangle$ can be obtained, in which n_b is the number of indistinguishable a–b interactions, and the summations are over b, as follows:

$$\cos\langle\phi\rangle \simeq [(\Sigma n_b \cos^2\phi_{ab}) / \Sigma n_b]^{1/2}$$

We estimated the error limits given for the number of scatterers, N, by varying σ [(*10*); Table 1] over a chemically reasonable range and indicate the range of N in which we expect the true values to lie.
17. J. J. Boland, S. E. Crane, J. D. Baldeschwieler, *J. Chem. Phys.* **77**, 142 (1982).
18. Part of this discord may arise because Klein and colleagues (*1–3*) interpolated $\alpha_{ab}(k)$ and $A_{ab}(k)$ from theoretical values (*11*); unfortunately such functions only poorly describe Mn–O model compound EXAFS, and similar difficulties have been found with iron [J. E. Penner-Hahn *et al.*, *J. Am. Chem. Soc.* **108**, 7819 (1986)]. Other contributing factors probably include the smaller k range and the lower signal-to-noise ratios of the data available to Klein and co-workers. In addition, their pronounced Fourier transform peak at $R + \Delta = 1.0$ Å (*1–3*) (not present in Fig. 1b) is most likely an artifact introduced by difficulties with baseline subtraction.
19. Simulations indicate that a spread in distances of 1.85 to 2.10 Å would reduce the apparent coordination number to about half of the true value.
20. B. Chiswell, E. D. McKenzie, L. F. Lindoy, in *Comprehensive Coordination Chemistry*, G. Wilkinson, R. D. Gillard, J. A. McCleverty, Eds. (Pergamon, Oxford, 1987), vol. 4, pp. 1–122.
21. O. Hansson, L.-E. Andreasson, T. Vanngard, *FEBS Lett.* **195**, 151 (1986); J. H. A. Nugent, *Biochim. Biophys. Acta.* **893**, 184 (1987).
22. G. W. Brudvig and R. H. Crabtree, *Proc. Natl. Acad. Sci. U.S.A.* **83**, 4586 (1986).
23. J. B. Vincent and G. Christou, *Inorg. Chim. Acta* **136**, L41 (1987).

24. The Stanford Synchrotron Radiation Laboratory is funded by the Department of Energy Office of Basic Energy Sciences and the National Institutes of Health Biotechnology Resource Program, Division of Research Resources.

23 August 1988; accepted 8 November 1988